Composite Structures 88 (2009) 624–628

Contents lists available at ScienceDirect

Composite Structures

journal homepage: www.elsevier.com/locate/compstruct

Material characterization of laminated composite materials using a three-point-bending technique

T.Y. Kam *, C.M. Chen, S.H. Yang

Mechanical Engineering Department, National Chiao Tung University, 1001 Ta Hsueh Road, Hsin Chu 300, Taiwan, ROC

ARTICLE INFO

Article history:
Available online 26 June 2008

Keywords:
A. Composite materials
A. Composite beam
C. Finite element method
C. Identification
C. Optimization
D. Experimental verification

ABSTRACT

A three-point-bending technique is presented for identifying the elastic constants of laminated composite materials. In the proposed technique, three strains in the axial, lateral, and 45° directions on the bottom surface at the mid-span of a symmetric angle-ply beam subjected to three-point-bending testing are measured for elastic constants identification. The narrow beam theory together with the trial elastic constants is used to predict the theoretical strains of the beam. The theoretical and experimental strains of the beams are then used in a stochastic optimization method to identify the elastic constants of the beam. The accuracy and applications of the proposed technique are demonstrated by means of a number of examples on the elastic constants identification of graphite/epoxy (Gr/ep) or glass/epoxy (Gl/ep) laminated composite materials. The effects of specimen aspect ratio and thickness on the accuracy of the proposed method are investigated.

1. Introduction

Material characterization is an important procedure in the developments of composite materials and components. According to ASTM D3039/3039M and D3518/3518M [1], three composite materials specimens with fiber angles of 0°, 90° and 45°, respectively, are used to determine four elastic constants, i.e., Young's modulus in fiber direction E_1, transverse Young's modulus E_2, shear modulus G_{12}, and Poisson's ratio v_{12} of the material. As well known, the specimen preparation and material testing processes are pretty time consuming, not to mention the cost. To shorten the time for material properties verification, a simple yet effective procedure that can expedite the material constants determination process is thus desired.

Recently, the determination of elastic constants of composite materials parts using measured system parameters has become an important topic of research [2–6]. For instance, Genovese et al. [2] proposed a hybrid numerical-experimental technique to identify the elastic constants of orthotropic materials using measured displacements. Liu et al. [3] presented a minimization method to determine the elastic constants of composite materials using measured elastic waves. In this paper, the material characterization of composites is also accomplished via an optimization approach. A simple yet effective three-point-bending technique is presented to determine the elastic constants of laminated composite materials. In the proposed technique, only one symmetric angle-ply beam specimen is needed to determine four elastic constants (E_1, E_2, G_{12}, and v_{12}) of the constituent composite material. The accuracy and applications of the proposed technique are demonstrated by means of several examples.

2. Strain analysis of symmetric angle-ply beam

The theoretical strains of the symmetric angle-ply beam with dimensions $b \times h \times L$ subjected to three-point bending as shown in Fig. 1 can be determined in the strain analysis of the beam based on the narrow beam theory [7]. The line load with intensity $\frac{F}{b}$ acting at the mid-span of the beam is distributed uniformly across the beam width. The stress resultant-curvature and strain-curvature relations of the beam are expressed, respectively, as

$$\begin{Bmatrix} M_x \\ 0 \\ 0 \end{Bmatrix} = \begin{bmatrix} D_{xx} & D_{xy} & D_{xs} \\ D_{yx} & D_{yy} & D_{ys} \\ D_{sx} & D_{sy} & D_{ss} \end{bmatrix} \begin{Bmatrix} \kappa_x \\ \kappa_y \\ \kappa_{xy} \end{Bmatrix} \tag{1}$$

and

$$\begin{Bmatrix} \varepsilon_x \\ \varepsilon_y \\ \gamma_{xy} \end{Bmatrix} = z \begin{Bmatrix} \kappa_x \\ \kappa_y \\ \kappa_{xy} \end{Bmatrix} \tag{2}$$

where $M_x = \frac{FL}{4b}$, the bending moment per unit width of the beam; κ_x, κ_y and κ_{xy} are curvatures in the x-direction, y-direction and x–y plane, respectively; ε_x, ε_y, and γ_{xy} are axial, lateral, and shear strains, respectively; z is the coordinate axis in thickness direction. It is noted that the expressions for evaluating the bending stiffness

* Corresponding author. Tel.: +886 3 5712121x55124; fax: +886 3 5753735.
E-mail address: tykam@mail.nctu.edu.tw (T.Y. Kam).

0263-8223/$ - see front matter © 2008 Elsevier Ltd. All rights reserved.
doi:10.1016/j.compstruct.2008.06.015

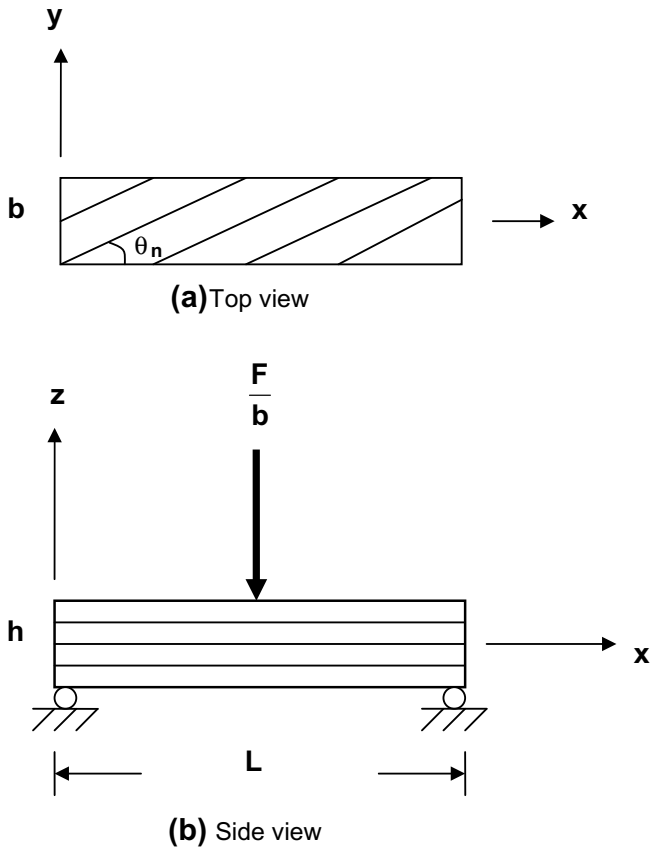

Fig. 1. Geometry and loading condition of symmetric angle-ply beam.

coefficients D_{ij}, which depend on the elastic constants and layer fiber angles of the beam, are available in the literature. The strains on the bottom surface at the mid-span of the beam can be determined by solving Eqs. (1) and (2).

$$\varepsilon_x = \frac{\mathrm{FLhd}_{xx}}{8b}$$
$$\varepsilon_y = \frac{\mathrm{FLhd}_{yx}}{8b} \qquad (3)$$
$$\gamma_{xy} = \frac{\mathrm{FLhd}_{sx}}{8b}$$

where d_{ij} are the flexibility coefficients. It is noted that the strains are dependent on the elastic constants of the beam.

When subjected to three-point bending, the symmetric angle-ply beam may twist and lift-offs may occur at the supported ends of the beam due to the existence of D_{sx} and D_{sy} in Eq. (1). Furthermore, for the beam with small shear modulus G_{23}, the across-thickness shear deformation may have certain effects on the deflection of the beam if its length-to-thickness ratio (L/h) is not large enough. Therefore, before proceeding to the material constants identification of the symmetric angle-ply beam, the applicability of the narrow beam theory should be validated and the appropriate dimensions of the beam determined. In the following validation study, the so-called beam is treated as a 2-D plate and the SHELL 99 element of the finite element code ANSYS [8], which has included the across-thickness shear effect in the formulation, is used to study the deformation of the $[(\theta^\circ/-\theta^\circ)_6]_s$ beam in Fig. 1. The dimensions of the plate are b × h × L (mm) and the intensity of the center line load is $\frac{3}{b}$ N/mm. Without loss of generality, the elastic constants of the composite material are set as E_1 = 146.5 GPa, E_2 = 9.22 GPa, $G_{12} = G_{13}$ = 6.84 GPa, $G_{23} = G_{12}/6$, ν_{12} = 0.3. In the finite element analysis, the translational degrees of freedom in z-direction at the two ends of the plate are initially restrained from movement. After applying the load to the plate, the translational degrees of freedom in the z-direction at the nodes with negative reactive nodal forces are released to allow movement. It is assumed that the load applicator is in complete contact with the whole width of the plate and the distribution of the applied load remains uniform during the loading process. The actual deformation of the plate is then determined via an iterative procedure in which the updated boundary conditions at the ends of the plate obtained in the previous iteration step are observed in formulating the finite element model of the plate at the present step. The iterative finite element analysis of the plate continues until the nodal reactive forces at the ends of the plate cease to change sign. The deformations of the symmetric angle-ply plates with L = 200 mm, h = 2.88 mm, and different widths and fiber angles have been studied in detail using the present iterative finite element method [9]. For instance, Fig. 2 shows the lift-off displacements at the left ends of the $[(45^\circ/-45^\circ)_6]_s$ plates with different aspect ratios (L/b) subjected to F=3 N. It is noted that the lift-off displacement decreases as the aspect ratio increases. In particular, the lift-off becomes negligible when $L/b \geqq 33.3$. The uniform across-the-width deflection at the mid-span of the plate obtained in the finite element analysis has validated the assumption of complete contact between the load applicator and the plate. It has been shown that at the mid-span of the plate with $\frac{L}{b} = 16.7$, the percentage differences of the strains predicted via the narrow beam and finite element approaches are less than 5% and they become much smaller as the plate's aspect ratio gets larger than 16.7. The across-thickness shear effects on the deformation of the angle-ply plates with different length-to-thickness ratios and fiber angles are also studied. For the plates with $\frac{L}{b} = 16.7$ and length-to-thickness ratios larger than 69, the small differences, which are less than 1%, between the deflections predicted by the 2-D finite element method and those by the narrow beam theory have demonstrated the insignificance of the shear effects. Therefore, for beams with aspect and length-to-thickness ratios larger than 16.7 and 69, respectively, the effects of lift-offs and across-thickness shear deformation on the strains of the beams can be neglected and the narrow beam theory is capable of predicting accurate strains for the beams. In the following elastic constants identification study, symmetric angle-ply beams with aspect and length-to-thickness ratios equal to 16.7 and 69, respectively, will be used to illustrate the feasibility and applications of the present method.

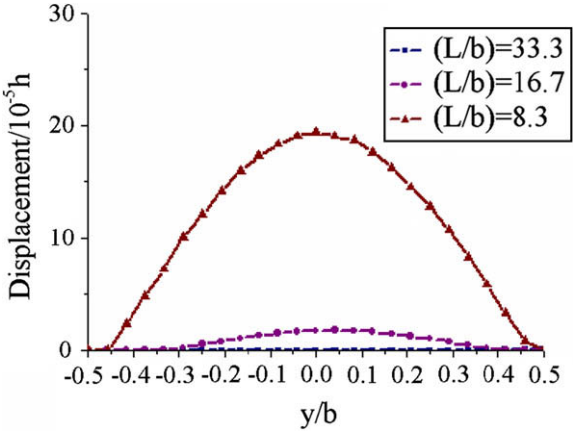

Fig. 2. Lift-off at the left end of the $[(45^\circ/-45^\circ)_6]_s$ beam.

3. Identification of elastic constants

The problem of elastic constants identification of a symmetric angle-ply beam is formulated as the following minimization problem.

$$\begin{aligned} &\text{Minimize } e(\underline{x}) = [(\varepsilon_x - \varepsilon_x^*)^2 + (\varepsilon_y - \varepsilon_y^*)^2 + (\gamma_{xy} - \gamma_{xy}^*)^2] \cdot \xi \\ &\text{Subject to } x_i^L \leqslant x_i \leqslant x_i^U; \quad i = 1{-}4 \end{aligned} \tag{4}$$

where $e(\underline{x})$ is the strain discrepancy function measuring the sum of the squared differences between the predicted and measured strains; $\underline{x} = [x_1 = E_1,\ x_2 = E_2,\ x_3 = G_{12},\ x_4 = \nu_{12}]$, the estimates of the elastic constants; ε_x^*, ε_y^*, and γ_{xy}^* are the measured axial, lateral, and shear strains, respectively; ξ is an amplification factor which is used to increase the sensitivity and avoid the occurrence of numerical underflow of the strain discrepancy function. A detailed numerical study has shown that for Gr/ep and Gl/ep materials, if the magnitudes of the strains are in the range from 10^{-4} to 10^{-6}, the value of ξ chosen in the range from 10^5 to 10^7 can help increase the convergence rate of the solution. x_i^L and x_i^U are the lower and upper bounds of the elastic constants, respectively. The predicted strains (ε_x, ε_y, and γ_{xy}) are determined from Eq. (3) for a given set of trial elastic constants. The above problem of Eq. (4) is then converted into an unconstrained minimization problem by creating the following general augmented Lagrangian.

$$\overline{\Psi}(\tilde{\underline{x}}, \underline{\mu}, \underline{\eta}, r_p) = e(\tilde{\underline{x}}) + \sum_{j=1}^{4} \left[\mu_j z_j + r_p z_j^2 + \eta_j \phi_j + r_p \phi_j^2\right] \tag{5}$$

with

$$\begin{aligned} z_j &= \max[g_j(\tilde{x}_{1j}), \tfrac{-\mu_j}{2r_p}] \\ g_j(\tilde{x}_j) &= \tilde{x}_{1j} - \tilde{x}_{1j}^U \leqslant 0 \\ \phi_j &= \max[H_j(\tilde{x}_{1j}), \tfrac{-\eta_j}{2r_p}] \\ H_j(\tilde{x}_j) &= \tilde{x}_{1j}^L - \tilde{x}_{1j} \leqslant 0 \quad j = 1 - 4 \end{aligned} \tag{6}$$

where μ_j, η_j, r_p are multipliers; max [*,*] takes on the maximum value of the numbers in the bracket. The modified design variables $\tilde{\underline{x}}$ are defined as

$$\tilde{\underline{x}} = \left[\frac{E_1}{\alpha_1}, \frac{E_2}{\alpha_2}, \frac{G_{12}}{\alpha_3}, \frac{\nu_{12}}{\alpha_4}\right] \tag{7}$$

A sensitivity study has shown that the normalization factors α_i, which are used to prevent E_1, E_2, and G_{12} from dominating the search direction of the solution and make all the modified design variables have appropriate contributions to the search direction, are chosen in such a way that they make the modified design variables less than 10 and greater than 0. The previously proposed stochastic global optimization method is then used to solve the above unconstrained minimization problem to find the best estimates of the elastic constants [10,11]. It is noted that in the adopted optimization method several starting points are randomly generated and for each starting point the lowest local minimum is searched. The solution converges when the probability of obtaining the global minimum reaches 0.995.

4. Experimental investigation

Two types of Gr/ep symmetric angle-ply beams with layups of $[(60°/-60°)_6]_s$ and $[(45°/-45°)_6]_s$ were fabricated for experimental study. The elastic constants of the cured Gr/ep material were first determined from testing using three types of the standard specimens of which each has 8 laminae in accordance with the ASTM standards of D3039 and D3518 and their average values and coefficients of variation (C.O.V.s) are given as follows.

$$\begin{aligned} E_1 &= 146.5 \text{ GPa } (0.7\%), \quad E_2 = 9.22 \text{ GPa } (1.2\%) \\ G_{12} &= 6.84 \text{ GPa } (3.2\%), \quad \nu_{12} = 0.3 \ (0.19\%) \end{aligned} \tag{8}$$

In the following study, the average values in the above equation are termed as the ASTM elastic constants of the composite material. The beam of aspect ratio $\frac{L}{b} = 16.7$ comprising 24 laminae of equal thickness in Fig. 3 was fabricated and cured under the same conditions used for preparing the standard specimens. In the three-point-bending testing of the beam, to minimize the average strain effects and get good approximations of strains at a specific point, three strain gages having gage length 3 mm and gage factor 2.08 ± 1.0% were used to measure the axial, lateral, and 45°-direction strains on the bottom surface at the mid-span of the beam. Herein, it is worth pointing out that the use of the three-point-bending test in this study is due to its simplicity. If more accurate strain measurements are desired, it is recommended to adopt the four-point-bending testing because the nearly uniform strain distributions along the span of the beam in-between the two loading points can greatly minimize the measurement errors induced by the gage-length effects of the strain gages. In the tests, the loading speed was set to be 0.01 mm/s. Once the three unit-directional strains were available, the shear strain at the same location was obtained as

$$\gamma_{xy}^* = 2\varepsilon_{45}^* - \varepsilon_x^* - \varepsilon_y^* \tag{9}$$

For each type of the symmetric angle-ply beams, three specimens were tested and the measured strains and their C.O.V.s are listed in Table 1. It is noted that the C.O.V.s of the measured strains are less than or equal to 2.1% and 1.2% for the $[(60°/-60°)_6]_s$ and $[(45°/-45°)_6]_s$ beams, respectively. The ASTM elastic constants were also used in the narrow beam theory to calculate the theoretical strains. In general, the experimental strains are larger than the corresponding theoretical ones and the percentage differences between the measured and theoretical strains given in the parentheses are less than or equal to 7.5%. The experimental strains are then used in the proposed identification method to determine the elastic constants of the beams.

5. Results and discussion

To demonstrate the feasibility and accuracy of the proposed elastic constants identification method, a number of numerical examples on the material characterization of Gr/ep or Gl/ep $[(\theta°/-\theta°)_6]_s$ beams with $\theta = 15$, 30, 45, and 60 subject to three-point bending are first considered. The actual elastic constants of the Gr/ep material are given in Eq. (8) while those of the Gl/ep material are 38.6 GPa, 8.27 GPa, 4.14 GPa, and 0.26 for E_1, E_2, G_{12}, and ν_{12}, respectively.

The value of the amplification factor in Eq. (4) is set to be 10^6. The upper and lower bounds of the elastic constants are chosen based on engineering judgment.

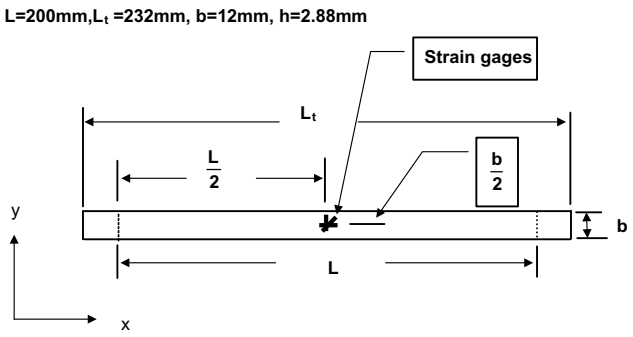

Fig. 3. Dimensions of beam specimen.

Table 1
Measured strains of Gr/ep $[(45°/-45°)_6]_s$ and $[(60°/-60°)_6]_s$ beams subject to $F = 3$ N

Specimen no.	Measured strains					
	$\varepsilon_x^*(10^{-4})$		$\varepsilon_y^*(10^{-4})$		$\gamma_{xy}^*(10^{-5})$	
	I[b]	II[c]	I[b]	II[c]	I[b]	II[c]
1	3.932 (+1.6%)[a]	7.002 (+1.2%)[a]	−2.775 (+1.3%)	−2.016 (+0.9%)	−1.321 (+2.4%)	−1.240 (+7.5%)
2	3.997 (+3.3%)	7.071 (+2.2%)	−2.821 (+3.0%)	−2.041 (+2.1%)	−1.350 (+4.7%)	−1.189 (+3.0%)
3	4.017 (+3.8%)	7.123 (+2.9%)	−2.841 (+3.7%)	−2.066 (+3.4%)	−1.341 (+4.0%)	−1.207 (+4.6%)
Average	3.982 (+2.9%)	7.065 (+2.1%)	−2.812 (+2.6%)	−2.041 (+2.1%)	−1.337 (+3.6%)	−1.212 (+5.0%)
C.O.V.	1.1%	0.9%	1.2%	1.2%	1.1%	2.1%

[a] Value in parentheses denotes the percentage difference between theoretical and measured strains.
[b] $[(45°/-45°)_6]_s$ beam.
[c] $[(60°/-60°)_6]_s$ beam.

Graphite/epoxy :
$0 < E_1 < 310$ GPa, $0 < E_2 < 20$ GPa, $0 < G_{12} < 20$ GPa, $0.1 < \nu_{12} < 0.5$
Glass/epoxy :
$0 < E_1 < 60$ GPa, $0 < E_2 < 16$ GPa, $0 < G_{12} < 16$ GPa, $0.1 < \nu_{12} < 0.5$ (10)

The normalization factors in Eq. (7) are chosen in such a way that the modified design variables for the elastic constants of Eq. (10) are within the following bounds.

$$\underline{\tilde{x}} = \left[0 < \frac{E_1}{\alpha_1} < 1.0, 0 < \frac{E_2}{\alpha_2} < 1.0, 0 < \frac{G_{12}}{\alpha_3} < 10, 0.1 < \frac{\nu_{12}}{\alpha_4} < 0.5\right] \quad (11)$$

In the numerical study, the theoretically derived strains are treated as the "measured" strains for identifying the elastic constants. Herein, the present method only uses five randomly generated starting points to identify the actual elastic constants of the composite materials. Furthermore, all the starting points can lead to the global minimum with numbers of iterations less than or equal to 10. For comparison purpose, the optimization algorithm DBCONF of IMSL [12] is also used to solve the minimization problem of Eq. (4) for determining the elastic constants of the Gr/ep and Gl/ep symmetric angle-ply beams. DBCONF, however, is unable to make the solutions converge and thus no results have been obtained. The first order second moment method [13] is also adopted to study the effects of measurement noise and fiber angle on the variations of the identified elastic constants. Among the beams under consideration, the $[(15°/-15°)_6]_s$ beam are less sensitive to the variations of the measured strains.

Now consider the elastic constants identification of the symmetric angle-ply beams which have been tested. The measured three strains of each of the $[(60°/-60°)_6]_s$ and $[(45°/-45°)_6]_s$ beams as well as their average values in Table 1 are used separately in the present method to identify the elastic constants of the beams. The estimates of E_1, E_2, G_{12}, and ν_{12} determined using different sets of measured strains are listed in Table 2. It is noted that for the three $[(60°/-60°)_6]_s$ beams, the percentage differences between the ASTM and identified elastic constants are less than or equal to 7.0%, 3.6%, 3.1%, 10.0% for, respectively, E_1, E_2, G_{12}, and ν_{12}. The high percentage difference of ν_{12} is mainly due to the small value of ν_{12} itself. It is also noted that amongst the identified elastic constants, the percentage difference of the identified shear modulus is the smallest. The C.O.V.s of the identified elastic constants are less than or equal to 3.61%. Compared to the maximum C.O.V. of 3.2% in Eq. (8), it is noted that both the ASTM and present method produce similar variations for the elastic constants. If the average measured strains are used in the identification method, the percentage differences of the estimates of E_1, E_2, G_{12}, and ν_{12} become 5.0%, 2.2%, 2.0% and 6.7%, respectively. Again it is noted that amongst the identified elastic constants, the percentage difference of the identified shear modulus is the smallest. Furthermore, the use of more specimens in the identification process can produce smaller percentage differences for the elastic constants. As for the $[(45°/-45°)_6]_s$ beams, the percentage differences between the ASTM and identified elastic constants are less than or equal to 4.2%, 8.5%, 3.7%, and 0.33% for, respectively, E_1, E_2, G_{12}, and ν_{12}. In this case, amongst the identified elastic constants, the percentage difference of the identified Poisson's ratio is the smallest. The C.O.V.s of the identified elastic constants are less than or equal to 3.86%. The similar C.O.V.s of the identified elastic constants produced by the $[(60°/-60°)_6]_s$ and $[(45°/-45°)_6]_s$ beams have demonstrated the consistency of the present method. If the average measured strains are used in the identification method, the percentage differences of the estimates of E_1, E_2, G_{12} and ν_{12} become 3.5%, 3.7%, 2.8% and, 0%, respectively. Again it is noted that amongst the identified elastic constants, the percentage difference of the identified Poisson's ratio is the smallest and the use of more specimens in the identification process can produce smaller percentage differences for the elastic constants. As indicated in the previous section on strain analysis of beams, more accurate results of elastic constants should be obtained for the symmetric angle-ply beams with aspect and length-to-thickness ratios larger than 16.7 and 69, respectively, because more accurate strains can be determined for such beams.

Table 2
Identified elastic constants of Gr/ep $[(45°/-45°)_6]_s$ and $[(60°/-60°)_6]_s$ beams using measured strains

Specimen no.	Identified elastic constant							
	E_1 (GPa)		E_2 (GPa)		G_{12} (GPa)		ν_{12}	
	I[b]	II[c]	I[b]	II[c]	I[b]	II[c]	I[b]	II[c]
1	142.84 (2.5%)[a]	140.92 (3.8%)[a]	9.05 (1.8%)	8.92 (3.3%)	6.74 (1.5%)	6.83 (0.1%)	0.301 (0.33%)	0.33 (10%)
2	141.35 (3.5%)	136.21 (7.0%)	8.44 (8.5%)	9.20 (0.2%)	6.63 (3.1%)	6.63 (3.1%)	0.300 (0%)	0.31 (3.3%)
3	140.33 (4.2%)	141.70 (3.3%)	9.01 (2.3%)	8.89 (3.6%)	6.59 (3.7%)	6.66 (2.6%)	0.300 (0%)	0.33 (10%)
Average	141.38 (3.5%)	139.2 (5.0%)	8.88 (3.7%)	9.02 (2.2%)	6.65 (2.8%)	6.70 (2.0%)	0.300 (0%)	0.32 (6.7%)
C.O.V.	0.89%	2.13%	3.86%	1.90%	1.17%	1.61%	0.19%	3.61%

[a] Value in parentheses denotes the percentage difference between the ASTM and identified elastic constants.
[b] $[(45°/-45°)_6]_s$ beam.
[c] $[(60°/-60°)_6]_s$ beam.

Table 3
Strains of angle-ply beam subjected to axial force of 100 N

Beam	$[(45°/-45°)_6]_s$			$[(60°/-60°)_6]_s$		
Strain	Experimental*	Theoretical		Experimental	Theoretical	
		(i)[a]	(ii)[b]		(i)	(ii)
$\varepsilon_x(10^{-6})$	130.32	123.6 (5.2%)[c]	127.27 (2.3%)	233.76	221.37 (5.6%)	225.95 (3.5%)
$\varepsilon_y(10^{-6})$	−89.98	−87.92 (−2.3%)	−90.29 (0.3%)	−66.03	−64.15 (−2.9%)	−65.45 (−0.9%)

* Average Strain obtained from 3 beam specimens.
[a] Strain predicted using ASTM elastic constants.
[b] Strain predicted using identified elastic constants.
[c] Percentage difference between experimental and theoretical strains.

In view of the material constants determined by the present and ASTM approaches, it is interesting to note that, except Possion's ratio, the identified material constants are less than their ASTM counterparts. This phenomenon implies that the composite material of the beams is 'weaker' than that of the ASTM specimens. Therefore, to further investigate the accuracy of the present material constants identification method, the beam specimens were subjected to tensile testing to measure the axial and lateral strains at the mid-span of the beams. The ASTM material constants and the material constants identified by the present method using the average measured strains are also used separately in the finite element analysis to predict the theoretical strains of the beams. Table 3 lists the experimental and analytical strains of the beams for comparison. It is noted that the strains predicted using the present identified material constants can match the experimental strains more closely than those predicted using the ASTM material constants. The degradations of the beam material constants might be caused by the imperfect curing in the relatively thick beams or other uncertain factors involved in the curing process.

6. Conclusions

A simple yet effective method for elastic constants identification of laminated composite materials using three strains of a symmetric angle-ply beam subjected to three-point-bending testing has been presented. The strains measured from the beam have been used in an optimization method to identify the elastic constants of the composite material. A numerical study has demonstrated the capability and accuracy of the present method in identifying the actual elastic constants of Gr/ep and Gl/ep symmetric angle-ply beams. Good estimations of the elastic constants can be obtained for the beams with aspect and length-to-thickness ratios larger than or equal to 16.7 and 69, respectively. A number of Gr/ep $[(60°/-60°)_6]_s$ and $[(45°/-45°)_6]_s$ beams have been subjected to three-point-bending and tensile tests to further demonstrate the accuracy and applications of the present method. It has been shown that when comparing with the ASTM procedure, the present identification method can predict more realistic material constants for the beams.

Acknowledgment

This research work was supported by the National Science Council of the Republic of China under Grant No. NSC 94-2212-E-009-020.

References

[1] ASTM. Standards and literature references for composite materials. 2nd Ed., West Conshohocken, Pa.; 1990.
[2] Genovese K, Lamberti L, Pappalettere C. A new hybrid technique for in-plane characterization of orthotropic materials. Exp Mech 2004;44(6):584–92.
[3] Liu GR, Ma WB, Han X. An inverse procedure for determination of material constants of composite laminates using elastic waves. Comput Methods Appl Mech Eng 2002;191:3543–54.
[4] Castagnède B, Jenkins JT, Sachse W, Baste S. Optimal determination of the elastic constants of composite materials from ultrasonic wave-speed measurements. J Appl Phys 1990;67(6):2753–61.
[5] Mota Soares CM, Moreira de Freitas M, Araújo AL, Pederson P. Identification of material properties of composite plate specimens. Compos Struct 1993;25:277–85.
[6] Sol H, Hua H, De Visscher J, Vantomme J, De Wilde WP. A mixed numerical/experimental technique for the nondestructive identification of the stiffness properties of fibre reinforced composite materials. NDT & E Int 1997;30(2):85–91.
[7] Swanson SR. Introduction to design and analysis with advanced composite materials. Upper Saddle River New Jersey (NJ): Prentice-Hall International Inc.; 1997.
[8] ANSYS, Documentation, Release 7.1, ANSYS Inc.; 2003.
[9] Chen CM. Elastic constants identification of laminated composite plate and beam structures. PhD dissertation, Mechanical Engineering Department, National Chiao Tung University, Taiwan; 2006 [in Chinese].
[10] Wang WT, Kam TY. Elastic constants identification of shear deformable laminated composite plates, ASCE. J Eng Mech 2001;127(11):1117–23.
[11] Snyman JA, Fatti LP. A multi-start global minimization algorithm with dynamic search trajectories. J Optim Theory Appl 1987;54(1):121–41.
[12] IMSL, User's manual, Version 3.0, IMSL Inc.; 1994.
[13] Benjamin JR, Cornell CA. Probability, statistics, and decision for civil engineers. New York: McGraw-Hill Companies Inc.; 1970.